The Canadian Mineralogist
Vol. 44, pp. 1331-1339 (2006)

CARYOCHROITE, A NEW HETEROPHYLLOSILICATE MINERAL SPECIES RELATED TO NAFERTISITE, FROM THE LOVOZERO MASSIF, KOLA PENINSULA, RUSSIA

PAVEL M. KARTASHOV§

Institute of Geology of Ore Deposits, Mineralogy, Petrology and Geochemistry, Russian Academy of Sciences, IGEM, Russian Academy of Sciences, Staromonetnyi per. 35, RU-109017 Moscow, Russia

GIOVANNI FERRARIS¶

Dipartimento di Scienze Mineralogiche e Petrologiche, Università di Torino, and Istituto di Geoscienze e Georisorse, CNR, Via Valperga Caluso, 35, I-10125 Torino, Italy

SVETLANA V. SOBOLEVA

Institute of Geology of Ore Deposits, Mineralogy, Petrology and Geochemistry, Russian Academy of Sciences, IGEM, Russian Academy of Sciences, Staromonetnyi per. 35, RU-109017 Moscow, Russia, and Dipartimento di Scienze Mineralogiche e Petrologiche, Università di Torino, Via Valperga Caluso, 35, I-10125 Torino, Italy

NIKITA V. CHUKANOV

Institute of Problems of Chemical Physics, RU-142432 Chernogolovka, Moscow Oblast, Russia

ABSTRACT

Caryochroite, a new mineral species, ideally $(Na,Sr)_3(Fe^{3+},Mg)_{10}[Ti_2Si_{12}O_{37}](H_2O,O,OH)_{17}$, is monoclinic, with cell parameters *a* 16.47, *b* 5.303, *c* 24.39 Å, β 93.5°, *Z* = 2. It was collected on the dumps of the Umbozero mine, Mount Alluaiv, Lovozero massif, Kola Peninsula, Russia. It is associated with albite, elpidite, epididymite, quartz, natrolite, pyrite, galena, sphalerite and bitumen. Caryochroite is the product of the supergene alteration of an unidentified Fe^{2+}-rich protophase; it forms centimetric crusts. Physical properties: submicrometric {001} lamellae, [010] elongate; opaque; hazel-brown color; pale brownish yellow streak; dull to waxy luster; hardness, 2½; good {001} cleavage; D_{meas} 2.990 g cm^{-3}; biaxial (–), α <1.700, β 1.745, γ 1.775, $2V_{meas}$ 75°; pleochroism: *X* = *Y* (dark brown) > *Z* (brown). The name refers to the color. Chemical data from electron microprobe, wet-chemical analysis for Fe and thermal analysis (9.17 wt% loss at 800°C); Mössbauer spectroscopy shows major Fe^{3+} and minor Fe^{2+}; the empirical formula is $(Na_{1.19}Sr_{0.62}Ca_{0.41}Mn_{0.35}K_{0.26})_{\Sigma 2.83}$ $(Fe^{3+}_{7.98}Mg_{1.15}Mn_{0.49}Fe^{2+}_{0.38})_{\Sigma 10.00}$ $(Ti_{1.87}Fe^{3+}_{0.13})_{\Sigma 2.00}$ $(Si_{11.74}Al_{0.26})_{\Sigma 12.00}$ $O_{54.10}H_{20.40}$. The spacing (Å) and intensity (%) of the strongest six lines of the X-ray powder-diffraction pattern are: 14.1(20), 13.3(30), 12.1(100), 4.38(10), 2.692(12), and 2.631(13). The cell parameters, X-ray powder-diffraction pattern, chemical composition and infrared spectrum suggest that caryochroite is the second heterophyllosilicate based on a nafertisite-type *HOH* layer. We evaluate the role of caryochroite and associated titano- and zirconosilicates as catalysts of the *in situ* formation of bitumen.

Keywords: caryochroite, new mineral species, heterophyllosilicates, nafertisite, titanosilicate, Kola Peninsula, Lovozero massif, bitumen catalysis.

SOMMAIRE

La caryochroïte, nouvelle espèce minérale de composition idéale $(Na,Sr)_3(Fe^{3+},Mg)_{10}[Ti_2Si_{12}O_{37}](H_2O,O,OH)_{17}$, est monoclinique, avec paramètres réticulaires *a* 16.47, *b* 5.303, *c* 24.39 Å, β 93.5°, *Z* = 2. On l'a trouvée dans les haldes de la mine Umbozero, mont Alluaiv, complexe de Lovozero, péninsule de Kola, en Russie. Lui sont associés albite, elpidite, épididymite, quartz, natrolite, pyrite, galène, sphalérite et bitume. La caryochroïte résulte d'une altération supergène d'un précurseur méconnu riche en Fe^{2+}; elle se présente en croûtes centimétriques. Propriétés physiques: lamelles submicrométriques {001}, allongement selon [010], opaque, couleur brun bistre, rayure jaune brunâtre pâle, éclat mat ou cireux, dureté 2½, clivage {001} assez bon,

§ *E-mail address*: pmk@igem.ru
¶ *E-mail address*: giovanni.ferraris@unito.it

D_{mes} 2.990; biaxe (–), α <1.700, β 1.745, γ 1.775, $2V_{mes}$ 75°; pléochroïsme: *X* = *Y* (brun foncé) > *Z* (brun). Le nom choisi fait allusion à la couleur. Les données chimiques ont été obtenues avec une microsonde électronique, complétées par analyse pour le Fe par voie humide, et analyse thermique (perte de 9.17% à 800°C). La spectroscopie de Mössbauer montre des proportions majeure de Fe^{3+} et mineure de Fe^{2+}. La formule empirique est $(Na_{1.19}Sr_{0.62}Ca_{0.41}Mn_{0.35}K_{0.26})_{\Sigma 2.83}$ $(Fe^{3+}_{7.98}Mg_{1.15}Mn_{0.49}Fe^{2+}_{0.38})_{\Sigma 10.00}$ $(Ti_{1.87}Fe^{3+}_{0.13})_{\Sigma 2.00}$ $(Si_{11.74}Al_{0.26})_{\Sigma 12.00}$ $O_{54.10}H_{20.40}$. Les valeurs de *d* (Å) et l'intensité (%) des six raies les plus intenses du spectre de diffraction X sur poudre sont: 14.1(20), 13.3(30), 12.1(100), 4.38(10), 2.692(12), et 2.631(13). D'après les paramètres réticulaires, le spectre de diffraction X (méthodes des poudres), la composition chimique et le spectre infrarouge, la caryochroïte serait le deuxième hétérophyllosilicate fondé sur une couche *HOH* de type nafertisite. Nous évaluons le rôle de la caryochroïte et des titanosilicates et zirconosilicates associés comme catalystes de la formation *in situ* du bitume.

(Traduit par la Rédaction)

Mots-clés: caryochroïte, nouvelle espèce minérale, hétérophyllosilicates, nafertisite, titanosilicate, péninsule de Kola, complexe de Lovozero, catalyse de la formation du bitume.

Introduction

In this paper, we report the occurrence and characterize the new mineral species caryochroite, ideally $(Na,Sr)_3(Fe^{3+},Mg)_{10}[Ti_2Si_{12}O_{37}](H_2O,O,OH)_{17}$. The species and mineral name have been approved by the IMA Commission on New Minerals and Mineral Names (IMA 2005–031). The name caryochroite is taken from the Greek κάρυον (nut) and χροιά (color) and recalls its hazel-brown color. The type material is labeled 3313/1 and deposited in the Fersman Mineralogical Museum of the Russian Academy of Sciences, Moscow, Russia.

Caryochroite likely represents the second layered titanosilicate species with a crystal structure based on a nafertisite-type layer. The objective of proving a close relationship between caryochroite and nafertisite has been reached by combining experimental data with the theory of the modular structures (*cf.* Ferraris *et al.* 2004). The main experimental data have been obtained by X-ray powder-diffraction (XRPD), electron-microprobe chemical analyses, Mössbauer and infrared (IR) absorption spectra, and transmission electron microscopy (TEM). Owing to the morphology of caryochroite, consisting of aggregates of very thin lamellae, no studies based on single-crystal X-ray diffraction were possible.

Background Information

The characterization of nafertisite, a rare titanosilicate first reported from the Khibina hyperagpaitic massif, in the Kola Peninsula, Russia (Khomyakov *et al.* 1995) and later from the Igaliko nepheline syenite complex, in South Greenland (Petersen *et al.* 1999), prompted Ferraris *et al.* (1996, 1997) to correlate a group of titanium silicates whose structures are based on phyllosilicate-like layers and to define the polysomatic series of the *heterophyllosilicates*. With reference to a *TOT* phyllosilicate layer, a row of Ti polyhedra periodically substitutes for a row of disilicate tetrahedra (silicate diorthogroups) in the *T* sheet of tetrahedra in members of the heterophyllosilicate series, whereas the *O* sheet of octahedra is maintained. Thus *HOH* layers are obtained, where *H* stands for *hetero* to indicate the presence of rows of 5- or 6-coordinated Ti (or replacing cations) in the *T* sheet of the layer silicates. The slice of the *HOH* layer containing rows of Ti polyhedra in its *H* sheet is conventionally called bafertisite-type module.

As summarized by Ferraris *et al.* (1997), depending on the periodicity of the hetero substitution and ignoring some minor topological features (*cf.* Nèmeth *et al.* 2005), three types of *HOH* layers are known so far (*cf.* Ferraris & Gula 2005).

$(HOH)_B$ bafertisite-type: A bafertisite-type module alone is periodically repeated; more than 30 minerals are based on this layer and belong to the so-called bafertisite mero-plesiotype series (Ferraris *et al.* 2001).

$(HOH)_A$ astrophyllite-type: Relative to the $(HOH)_B$ layer, a one-chain-wide mica-like module *M* is inserted in an astrophyllite-type layer between two bafertisite-type modules. About ten minerals are based on this layer and form an isomorphous series (Piilonen *et al.* 2003a, b). Presumably, eveslogite (Men'shikov *et al.* 2003) is based on the same layer.

$(HOH)_N$ nafertisite-type: Relative to the $(HOH)_B$ layer, two one-chain-wide mica-like modules *M* are inserted in a $(HOH)_N$ nafertisite-type layer between two bafertisite-type modules. Only nafertisite $\{(Na,K,\square)_4(Fe^{2+},Fe^{3+},\square)_{10}[Ti_2O_3Si_{12}O_{34}](O,OH)_6$; *A*2/*m*, *a* 5.353, *b* 16.176, *c* 21.95 Å, β 94.6°$\}$ has been described as based on this layer (Fig. 1; Ferraris *et al.* 1996). The new species caryochroite belongs to this type.

Occurrence

Specimens of caryochroite were collected on dumps transported from the hydrothermal zone of the Elpiditovyi pegmatite of the Umbozero mine at Mount Alluaiv, in the northwestern sector of the Lovozero massif, Kola Peninsula, Russia. This pegmatite is a tube-like formation situated among rocks of the differentiated complex (foyaites and urtites) and has been described by Pekov (2000), who mentioned an "undetermined ferroan hydrosilicate" intercalated with elpidite. In small cavities and fissures of the albite zone in the pegmatite, spheroids of caryochroite overgrow

albite, quartz, pyrite and epididymite. In the central large cavity of the pegmatite, caryochroite forms large massive crusts on, and intercalated with, elpidite. Associated minerals are: albite, elpidite, epididymite, quartz, natrolite, pyrite, galena, sphalerite, bitumen.

Caryochroite is the product of supergene alteration (oxidation and dehydration) of a Fe^{2+}-rich protophase locally known as "amorphous greenish grey mineral" for which a satisfactory characterization is not yet available. This phase is unstable: after contact with air, its dark green color changes rapidly to brown because of oxidation of the iron. The protophase has been noted in the core of massive samples of caryochroite extracted from a depth of about 0.5 m in 2002 and 2003, but soon it transformed to caryochroite. Holotype and cotype specimens collected at the same time (1991) and preserved at room conditions are completely oxidized and do not contain relics of the protophase.

Spheroids of bitumen are included in caryochroite and overgrow both it and elpidite. The presence of bitumen and pyrite are indicative of reducing conditions, which *in situ* stabilize the Fe^{2+}-rich caryochroite protophase. Spatial relationships among the species show that protophase formed at a low-temperature hydrothermal stage, possibly from stagnant meteoric waters filling the central cavity of the pegmatite. The order of crystallization of the main minerals is: albite, natrolite, elpidite, caryochroite protophase.

Appearance and Physical Properties

Caryochroite spherules are millimetric and form crusts up to 5 × 5 × 0.2 cm (Fig. 2) [and even up one meter in the original pegmatite, according to Igor V. Pekov (pers. commun.)] within cavities and on the surface of albite; the concretion-like morphology is inherited from the protophase and does not show zoning. Some larger (more than 10 cm in size) cork-like masses contain clusters of thin needles of elpidite (up to 4 cm long). Single crystals are observable only by electron microscopy (Fig. 3; see below).

Caryochroite is opaque and shows a dull to waxy luster; its megascopic color is hazel brown; the streak is pale brownish yellow. No fluorescence was observed. The Mohs hardness of the aggregates is 2.5. The mineral shows a good {001} cleavage, no parting, and a conchoidal fracture; aggregates are ductile. The measured density (suspension in aqueous solution of Clerici liquid) is 2.990(5); on the basis of the cell parameters and chemical composition given below, the calculated density is 3.076 g/cm^3. The smaller value of the measured density is related to the presence of micrometric cavities in the grains of caryochroite.

At a wavelength of 589 nm, caryochroite is biaxial (–), with $\alpha < 1.700$, β 1.745(5) and γ 1.775(5), $2V_{meas}$ 75(10)°. From the measured values of β, γ and $2V$, a value of 1.687 is calculated for α. The orientation is: $Y // x$ and $Z // y$, *i.e.*, β and γ are in the plane (001). The values of the $X \wedge z$ angle and of α could not be measured because the lamellae are very thin. No dispersion has been observed because the mineral is dark brown in thin section. Pleochroism: $X = Y > Z$, with Z brown, X and Y dark brown.

The Chemical Composition of Caryochroite

The information on the chemical composition and the crystal-chemical characteristics of caryochroite have been obtained by several methods. In particular, the presence of major Fe^{3+} and only minor Fe^{2+} and the structural relationship with nafertisite have been established by Mössbauer and infrared (IR) absorption spectroscopy.

Infrared absorption spectroscopy

The IR spectrum of caryochroite (Fig. 4) shows bands at the following wavenumbers (cm^{-1}, s: strong, w: weak, sh: shoulder): 3510 s, 3405 s, 3250 sh, 1630, 1420 w, 1023 s, 981 s, 940 s, 765 w, 667, 570 sh, 443 s. The maximum at 3510 cm^{-1} tends to become a shoulder at about 3500 cm^{-1} in samples kept in the laboratory. However, in all samples, the integral intensity of the broad band at 3405 cm^{-1} is much higher than the intensity of the band in the range 3500–3510 cm^{-1}, *i.e.*, H_2O strongly prevails over OH^-. The presence of CO_2 is not shown by the IR spectrum.

Thermal analysis

DTA and TGA analyses (Fig. 5) have been performed in the interval of temperature 20–1000°C on 420 mg of caryochroite, at a heating rate of 10°C per minute in a nitrogen atmosphere. The corresponding curves present two endothermic effects: a broad one in the interval 100–490°C, with a maximum at 240°C, and a sharper one in the interval 490–600°C, with a maximum at 505°C. The DTA curve presents also three small exothermic effects, at temperatures higher than 700°C, which likely are due to recrystallization processes; the largest of these effects leads to the peak at 770°C. The weight loss of 1.31% in the range 20–100°C is attributed to surface-adsorbed water and is not taken into account in the chemical composition (Table 1); the 7.50 (100–490°C) and 1.67 wt.% losses (490–800°C), for a total of 9.17 wt.%, are attributed to molecular H_2O and hydroxyl groups, respectively.

Mössbauer spectroscopy

Figure 6 shows the Mössbauer spectrum of caryochroite. It has been collected at room temperature in transmission mode on a 100 mg sample with a mean particle-size of 0.05 mm using a ^{57}Co (Cr matrix) source, with a constant-acceleration MS–1104EM spectrometer. The spectrum could be unambiguously

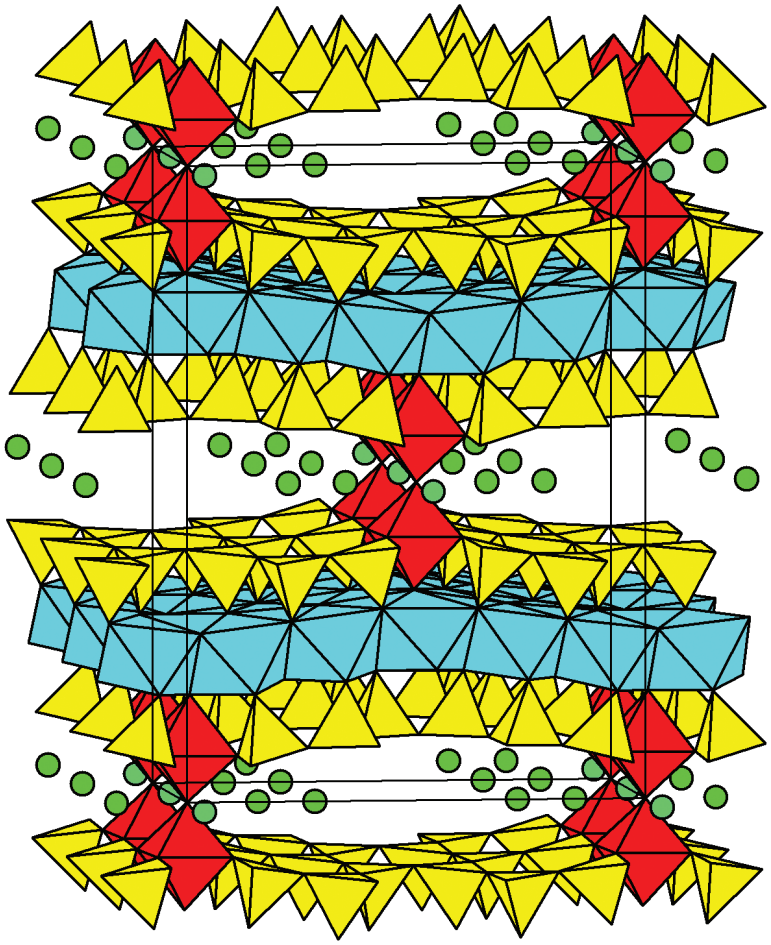

FIG. 1. Clinographic view along [010] of the crystal structure of nafertisite (atom coordinates from Ferraris *et al*. 1996). Yellow tetrahedra and red octahedra form the *H* sheets; the *O* sheets consist of blue octahedra.

fitted with two Lorentzian quadrupole doublets for Fe^{3+} and one for Fe^{2+}. The values of the isomer shifts and quadrupole splittings (Table 2) show that all the Fe occupies differently distorted octahedral sites. From the areas of the fitted doublets, we infer that Fe^{2+} represents about 7(2) % of the total iron, a value to be compared with that of 15% obtained by wet-analysis (see below). Presumably, the significant difference is related to the different method of preparation of the samples.

Chemical composition

We have analyzed caryochroite with an energy-dispersion spectrometer (EDS) and an electron microprobe (JSM 5300 Link ISIS) operating at 25 kV and <1 nA; each of five point-analyses was taken over a scanned area of 2000 × 1500 μm. The Fe^{3+} and Fe^{2+} contents have been determined by wet-chemical analysis (Table 1). A chemical analysis by X-ray fluorescence (results not reported) showed wt.% values very close to those found with the electron microprobe.

By analogy with nafertisite (see Discussion), the following empirical formula is obtained from the data of Table 1 on the basis of Si + Al = 12 atoms per formula unit (*apfu*):

$$(Na_{1.19}Sr_{0.62}Ca_{0.41}Mn_{0.35}K_{0.26})_{\Sigma 2.83}(Fe^{3+}_{7.98}Mg_{1.15}Mn_{0.49}Fe^{2+}_{0.38})_{\Sigma 10.00}(Ti_{1.87}Fe^{3+}_{0.13})_{\Sigma 2.00}(Si_{11.74}Al_{0.26})_{\Sigma 12.00}O_{54.10}H_{20.40}.$$

As both IR and thermal analysis data show H_2O largely dominant over OH, a nafertisite-type formula for

caryochroite can be idealized as $(Na,Sr)_3(Fe^{3+},Mg)_{10}[Ti_2Si_{12}O_{37}](H_2O,O,OH)_{17}$.

Crystallographic Data

With a transmission electron microscope (Philips CM12), we are able to show that single crystals have dimensions of about 0.1 × 1.0 μm only and appear as {001} lamellae, which are developed along their [010] direction (Fig. 3). The (*hk*0) selected-area electron-diffraction (SAED) patterns (not reported) show *mm* symmetry and allow us to obtain approximate values of the *a* and *b* cell parameters, which have been used to index the X-ray powder-diffraction pattern (Table 3). From this pattern, the following refined unit-cell parameters have been obtained: *a* 16.47(2), *b* 5.303(6), *c* 24.39(3) Å, β 93.5(2)°, *V* 2126 Å^3. The monoclinic cell contains two formula units ($Z = 2$) with the composition given below. The value of the compatibility index $[1 - (K_P/K_C)]$ is 0.042 (good) with $D_{meas} = 2.990$ and 0.015 (superior) for $D_{calc} = 3.076$.

Discussion

The overall aspect of the X-ray powder-diffraction pattern of caryochroite, which is dominated by one strong peak at low angles, the values of cell parameters, and the silicate part of the chemical composition are features comparable with those of the titanosilicate nafertisite (Ferraris *et al*. 1996, Khomyakov *et al*. 1995) and sepiolite (Brauner & Preisinger 1958) (Table 4).

On the basis of the following discussion, the infrared spectrum (Fig. 4) of caryochroite favors a relationship to nafertisite more than to sepiolite. For aluminosilicates with an anion stoichiometry $Si_xAl_yO_z$, Chukanov (1995) proposed the following correlation between the weighted average frequency $\langle\nu_{Si-O}\rangle$ (cm^{-1}) of the Si–O-stretching vibrations and the parameter $t = z(x + y/2)^{-1}$:

$$\langle\nu_{Si-O}\rangle = (337.8t + 1827)(0.6428t + 1)^{-1}.$$

Note that as defined, the parameter *t* increases with a decrease in the mean number of vertices shared between the SiO_4 tetrahedra, because the coefficient *z* increases in the stoichiometric formula of the anion. The continuous sheet of tetrahedra in sepiolite implies that each tetrahedron shares three vertices with other tetrahedra: thus, $t = 2.5$ is obtained. Instead, in nafertisite, the sheet of tetrahedra is interrupted by the insertion of Ti-bearing octahedra (Fig. 1). Consequently, *t* is equal to 2.83. For both caryochroite and nafertisite, the measured value of $\langle\nu_{Si-O}\rangle$ is 990 cm^{-1}, close to the value of 987 cm^{-1} calculated for the anion $Si_{12}O_{34}$ ($t = 2.83$). Instead, in sepiolite-type minerals, the measured $\langle\nu_{Si-O}\rangle$ value is in

FIG. 2. Sample of caryochroite (real dimensions 5 × 6 cm).

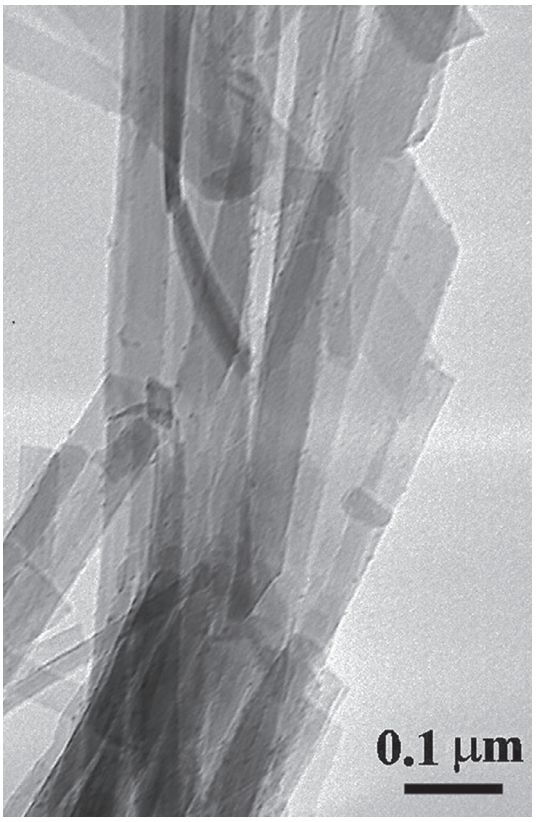

FIG. 3. Transmission electron microscopy (TEM) image of caryochroite lamellae.

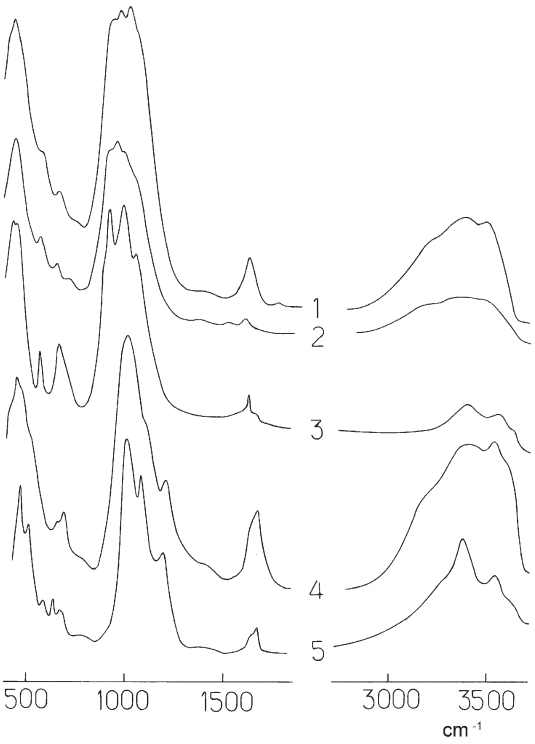

FIG. 4. Infrared (IR) spectra of caryochroite (1); nafertisite from the Nanna pegmatite, Igaliko, Greenland (2); holotype nafertisite from Kukisvumchorr Mt., Khibiny, Kola (3); sepiolite with Mg:Fe = 1.48 from Tyrol, Austria (4); Fe-dominant (almost Mg-free) analogue of sepiolite from Flora Mountain, Lovozero, Kola (5).

the range 1015–1030 cm^{-1} (Fig. 4), and that calculated for the anion $Si_{12}O_{30}$ (t = 2.5) is 1025 cm^{-1}. Besides, in the IR spectrum of sepiolite, an absorption band in the range 1160–1220 cm^{-1} is present and corresponds to stretching vibrations of Si–O–Si linkages situated at the inversions in the sheet of tetrahedra. In the IR spectra of nafertisite and caryochroite, this band is absent. Thus, besides the crystallographic data mentioned above, the features of the IR spectra of caryochroite and nafertisite also support a similarity between the crystal structures of these two minerals.

Concerning the crystal-chemical relationships between caryochroite and nafertisite, it is useful to consider the general formula for a nafertisite-type member of the heterophyllosicates series (*cf.* Ferraris *et al.* 2004): $I_4Y_{10}[Ti_2(O')_3Si_{12}O_{34}](O")_6$. In this formula, atoms belonging (even in part) to the *H* sheet of the *HOH* layer described under Background Information are shown in square brackets. *I* and *Y* are interlayer and octahedrally coordinated cations, respectively; O' (bonded to *Ti*) and O" (belonging to the *O* sheet of octahedra only) can be O, OH, F or H_2O; the 34 atoms of oxygen in the $Si_{12}O_{34}$ group are bonded to Si. In comparison with the expected formula, the given idealized formula of caryochroite shows 17 O" instead of 6 O", with O" representing (H_2O,O,OH). Reasonably, the content of hydrogenated oxygen atoms exceeding 6 O" can be accommodated in the interlayer of a nafertisite-like structure (Fig. 1). Following the analogy with the expected formula and findings in other heterophyllosilicates (*e.g.*, Ferraris & Gula 2005), a minor part of Fe^{3+} has been indicated as replacing Ti in the empirical formula of caryochroite given above. The total Mn has instead been distributed between the *O* sheet and the interlayer, because crystal-chemically, Mn^{2+} can behave as Ca, which is a typical interlayer cation in heterophyllosilicates.

The area of the *ab* base in caryochroite (87.18 $Å^2$) is slightly larger than that in nafertisite (86.60 $Å^2$), in spite of the fact that the *O* sheet is occupied by smaller cations (Fe^{3+}) in the new mineral (Table 4). However, a realistic comparison should take into account also the thickness of the *O* sheets, which is unknown in caryochroite, and the ionic radii of the anions, which in nafer-

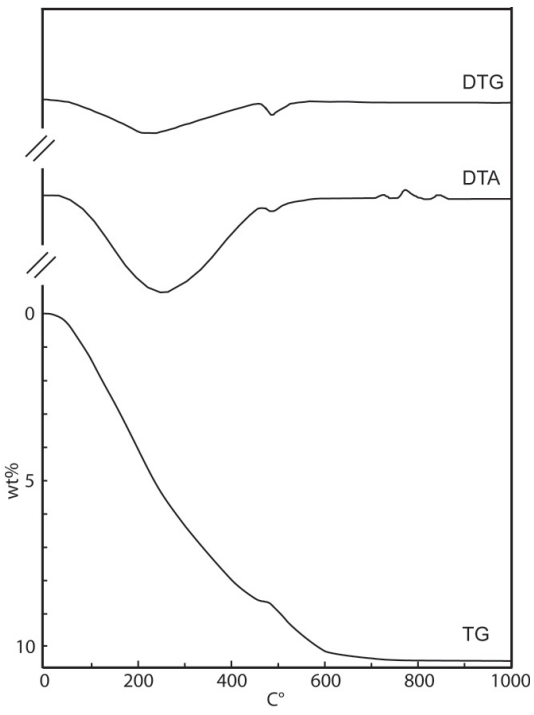

FIG. 5. Differential thermal gravimetry (DTG), differential thermal analysis (DTA) and thermogravimetric (TG) curves for caryochroite.

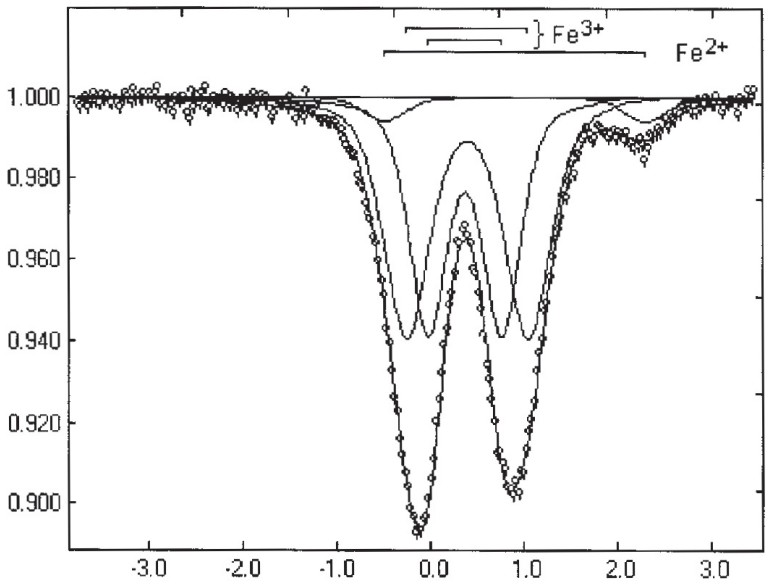

FIG. 6. Mössbauer spectrum of caryochroite. The separations between the components of the Fe^{3+} (two) and Fe^{2+} (one) doublets used to fit the experimental data are shown at the top. Horizontal and vertical axes show velocity (mm/s) and relative transmission, respectively.

TABLE 1. CHEMICAL DATA FOR CARYOCHROITE

	Wt.%	Range	Probe standard
SiO_2	35.20	34.71 – 35.46	Chkalovite
TiO_2	7.47	7.24 – 7.65	$MgTiO_3$
Al_2O_3	0.66	0.52 – 0.76	Al metallic
MgO	2.32	2.12 – 2.76	$MgTiO_3$
CaO	1.15	1.05 – 1.21	Nacaphite
SrO	3.21	2.65 – 4.11	$SrSO_4$
MnO	2.98	2.86 – 3.14	Mn metallic
Fe_2O_3	32.31*		
FeO	1.35*	30.21 – 30.90*	Fe metallic
Na_2O	1.84	1.78 – 1.92	Nacaphite
K_2O	0.61	0.50 – 0.70	Orthoclase
H_2O	9.17**	–	
Sum	98.27		

* Proportion of Fe_2O_3 and FeO according to results of wet-chemical analysis; the range given pertains to the amount of FeO measured with an electron microprobe.
** Amount of H_2O determined by thermogravimetric analysis.

tisite are in part $(OH)^-$, whereas in caryochroite they are mainly O^{2-} to compensate the presence of Fe^{3+}.

CONCLUSIONS

The preservation of traces of the protophase in samples collected at some depth and their rapid disappearance at laboratory conditions show that, at the natural conditions of lower temperature and higher humidity, the transformation protophase → caryochroite is very slow. As a function of the freshness of the sample, a modification of the IR absorption band in the interval 3500–3510 cm^{-1}, which is due to stretching of weakly hydrogen-bonded $(OH)^-$ groups, has been observed in laboratory. That finding supports the proposal that coupled reactions $Fe^{2+} \rightarrow Fe^{3+}$ and $(OH)^- \rightarrow O^{2-}$ accompany the transformation.

The characterization of caryochroite largely benefitted from the modular (Ferraris *et al*. 2004) classification of the heterophyllosilicates (Ferraris *et al*. 1996, 1997) and the capability of infrared spectra of revealing common structural features that occur in different minerals (Chukanov 1995). The discovery of caryochroite shows that the number of mineral species with a crystal structure based on a nafertisite-type *HOH* layer may well expand, even if the poor crystallinity of these minerals will hinder their identification.

The hydrothermally altered Elpiditovyi pegmatite shows outstanding examples of association between bitumen and microporous titano- and zirconosilicates in alkaline hydrothermally modified rocks (Chukanov *et al*. 2005). As discussed by Chukanov & Pekov (2005) and Pekov & Chukanov (2005) for similar cases, caryochroite and elpidite may have acted as catalysts by facilitating the conversion of low-weight organic compounds to bitumen. This aspect may lead

TABLE 2. MÖSSBAUER DATA FOR CARYOCHROITE

Ion	Isomer shift (mm/s)	Quadrupole splitting (mm/s)	Line width (mm/s)	Relative intensity (%)
[a] Fe^{3+}	0.39(1)	1.25(1)	0.58(2)	52(2)
[b] Fe^{3+}	0.37(1)	0.73(1)	0.48(2)	41(2)
[c] Fe^{2+}	1.00(1)	2.76(1)	0.53(2)	7(2)

[a] Top bar in the upper part of Figure 4. [b] Intermediate bar in the upper part of Figure 4. [c] Bottom bar in the upper part of Figure 4.

TABLE 3. X-RAY POWDER-DIFFRACTION PATTERN OF CARYOCHROITE*

d(obs) (Å)	*I*(obs)	*d*(calc) (Å)	*hkl*
14.1	20	14.03	$\bar{1}01$
13.3	30	13.25	101
12.1	100	12.17	002
4.38	10	4.409	$\bar{2}11$
3.885	6	3.921, 3.852	$\bar{1}14$, 213
2.968	8	2.984, 2.979, 2.967	$\underline{5}03$, $\bar{4}06$, 413
2.923	8	2.925, 2.912	$\bar{4}14$, $\bar{2}08$
2.692	12	2.695, 2,693	$\bar{1}09$, 512
2.631	13	2.639, 2.636	602, 021
2.575	8	2.584, 2.564	118, $\bar{1}22$
2.507	6	2.505, 2.498	221, $\bar{1}23$
2.450	5	2.443	604
1.583	5	1.585, 1.582, 1.581	433, $\bar{3}0\underline{15}$, 818
1.543	7	1.542, 1.543, 1.541	$\bar{1}0\underline{14}$, 336, $\bar{9}18$
1.531	8	1.532, 1.531, 1.530	62$\underline{10}$, 30$\underline{15}$, $\bar{1}2\underline{13}$

* Siemens D-5000 diffractometer, Cu$K\alpha$ radiation (λ = 1.5418 Å).

TABLE 4. COMPARISON OF CARYOCHROITE WITH RELATED MINERALS

	Caryochroite	Nafertisite	Sepiolite
Formula	$(Na,Sr)_3$ $(Fe^{3+},Mg)_{10}$ $[Ti_2Si_{12}O_{37}]$ $(H_2O,O,OH)_{17}$	$(Na,K,\square)_4$ $(Fe^{2+},Fe^{3+},\square)_{10}$ $[Ti_2O_2Si_{12}O_{34}]$ $(O,OH)_6$	Mg_8 $[Si_{12}O_{30}]$ $(OH)_4 \bullet H_2O$
Crystal data	Monoclinic, *a* 16.47, *b* 5.303, *c* 24.39 Å, β 93.5°	Monoclinic, *A*2/*m*, *a* 5.353, *b* 16.176, *c* 21.95 Å, β 94.6°	Orthorhombic, *Pncn*, *a*13.40, *b* 26.80, *c* 5.28 Å
Strongest lines (Å)	14.1(20), 13.3(30), 12.1(100), 4.38(10), 2.692(12), 2.631(13)	13.00(30), 10.94(100), 4.45(15), 2.798(25), 2.641(20)	12.05(100), 4.306(40), 3.750(30), 3.366(30), 2.560(50)
Optics	α < 1.700, β 1.745, γ 1.775, (–), 2*V* 75°	α 1.627, β 1.667, γ 1.693, (–), 2*V* 75°	α 1.514, β 1.526, γ 1.527, (–), 2*V* 30°
Color	Hazel brown	Light green	White
Morphology	Concretion (mega), (001) lamellae [010] elongate (micro)	[100] fibrous (mega), (001) lamellar (micro)	[001] lamellar

to technological applications of these mineral phases whose structures show cavities and channels (pores) that are surrounded by different kinds of coordination polyhedra. These heteropolyhedral structures attract increasing attention for their properties similar to those of the zeolites where, instead, the pores are embedded in a framework of tetrahedra only (*cf*. Ferraris & Merlino 2005).

ACKNOWLEDGEMENTS

The contributions of P. Nèmeth (TEM), V.V. Korovushkin (Mössbauer), A.E. Zadov (optics) and I.V. Pekov (occurrence) are gratefully acknowledged. The constructive comments of the referees (E. Sokolova and R. Frost), associate editor (A.M. McDonald) and editor (R.F. Martin) helped to improve contents and the form of this article. This work was financially supported by MIUR (Roma, PRIN project 'Minerals to materials: crystal chemistry, microstructures, modularity, modulations') and Russian Foundation for Basic Research (grant #04–05–64085). Visits to Italy by S.V.S. were made possible by grants of MAE (Roma) and Università degli Studi di Torino, in the framework of Italian–Russian scientific and technological agreements.

REFERENCES

BRAUNER, K. & PREISINGER, A. (1958): Struktur und Entstehung des Sepioliths. *Tschermaks Mineral. Petrogr. Mitt.* **6**, 120-140.

CHUKANOV, N.V. (1995): On infrared spectra of silicates and aluminosilicates. *Zap. Vser. Mineral. Obshchest.* **124**(3), 80-85 (in Russ.).

CHUKANOV, N.V., ERMOLAEVA, V.N., PEKOV, I.V., SOKOLOV, S.V., NEKRASOV, A.N. & SOKOLOVA, M.N. (2005): Rare-metal mineralization connected with bituminous matters in late assemblages of pegmatites of the Khibiny and Lovozero massifs. *New Data on Minerals* **40**, 80-95.

CHUKANOV, N.V. & PEKOV, I.V. (2005): Heterosilicates with tetrahedral–octahedral frameworks: mineralogical and crystal-chemical aspects. *In* Micro- and Mesoporous Mineral Phases (G. Ferraris & S. Merlino, eds.). *Rev. Mineral. Geochem.* **57**, 105-145.

FERRARIS, G. & GULA, A. (2005): Polysomatic aspects of microporous minerals – heterophyllosilicates, palysepioles and rhodesite-related structures. *In* Micro- and Mesoporous Mineral Phases (G. Ferraris & S. Merlino, eds.). *Rev. Mineral. Geochem.* **57**, 69-104.

FERRARIS, G., IVALDI, G., KHOMYAKOV, A.P., SOBOLEVA, S.V., BELLUSO, E. & PAVESE, A. (1996): Nafertisite, a layer titanosilicate member of a polysomatic series including mica. *Eur. J. Mineral.* **8**, 241-249.

FERRARIS, G., IVALDI, G., PUSHCHAROVSKY, D.YU., ZUBKOVA, N.V. & PEKOV, I.V. (2001): The crystal structure of delindeite, $Ba_2\{(Na,K,\square)_3(Ti,Fe)[Ti_2(O,OH)_4Si_4O_{14}](H_2O,OH)_2\}$, a member of the mero-plesiotype bafertisite series. *Can. Mineral.* **39**, 1307-1316.

FERRARIS, G., KHOMYAKOV, A.P., BELLUSO, E. & SOBOLEVA, S.V. (1997): Polysomatic relationship in some titanosilicates occurring in the hyperagpaitic alkaline rocks of the Kola Peninsula, Russia. *Proc. 30th Int. Geol. Congress* **16**, 17-27.

FERRARIS, G., MAKOVICKY, E. & MERLINO, S. (2004): *Crystallography of Modular Materials*. IUCr/Oxford University Press, Oxford, U.K.

FERRARIS, G. & MERLINO, S., eds. (2005): Micro- and mesoporous mineral phases. *Rev. Mineral. Geochem.* **57**.

KHOMYAKOV, A.P., FERRARIS, G., NECHELYUSTOV, G.N., IVALDI, G. & SOBOLEVA, S.V. (1995): Nafertisite $Na_3(Fe^{2+},Fe^{3+})_6[Ti_2Si_{12}O_{34}](O,OH)_7 \bullet 2H_2O$, a new mineral with a new type of band silicate radical. *Zap. Vser. Mineral. Obshchest.* **124**(6), 101-108 (in Russ.).

MEN'SHIKOV, YU.P., KHOMYAKOV, A.P., FERRARIS, G., BELLUSO, E., GULA, A. & KULCHITSKAYA, E.A. (2003): Eveslogite, $(Ca,K,Na,Sr,Ba)_{48}[(Ti,Nb,Fe,Mn)_{12}(OH)_{12}Si_{48}O_{144}](F,OH,Cl)_{14}$, a new mineral from the Khibina alkaline massif, Kola Peninsula, Russia. *Zap. Vser. Mineral. Obshchest.* **132**(1), 59-67 (in Russ.).

NÈMETH, P., FERRARIS, G., RADNÓCZI, G. & AGEEVA, O.A. (2005). TEM and X-ray study of syntactic intergrowths of epistolite with murmanite and shkatulkalite. *Can. Mineral.* **43**, 973-987.

PEKOV, I.V. (2000). *Lovozero Massif: History, Pegmatites, Minerals*. Ocean Pictures Ltd., Moscow, Russia.

PEKOV, I.V. & CHUKANOV, N.V. (2005): Microporous framework silicate minerals with rare, and transition elements: minerogenetic aspects. *In* Micro- and Mesoporous Mineral Phases (G. Ferraris & S. Merlino, eds.). *Rev. Mineral. Geochem.* **57**, 145-171.

PETERSEN, O.V., JOHNSEN, O., CHRISTIANSEN, C.C., ROBINSON, G.W. & NIEDERMAYR, G. (1999): Nafertisite – $Na_3Fe_{10}Ti_2Si_{12}(O,OH,F)_{43}$ – from the Nanna Pegmatite, Narsaarsuup Qaava, South Greenland. *Neues Jahrb. Mineral., Monatsh.,* 303-310.

PIILONEN, P.C., LALONDE, A.E., MCDONALD, A.M., GAULT, R.A. & LARSEN, A.O. (2003a): Insights into astrophyllite-group minerals. I. Nomenclature, composition and development of a standardized general formula. *Can. Mineral.* **41**, 1-26.

PIILONEN, P.C., MCDONALD, A.M. & LALONDE, A.E. (2003b): Insights into astrophyllite-group minerals. II. Crystal chemistry. *Can. Mineral.* **41**, 27-54.

Received February 20, 2006, revised manuscript accepted June 22, 2006.